Tianjin Daxue Xuebao (Ziran Kexue yu Gongcheng Jishu Ban)/
Journal of Tianjin University Science and Technology
ISSN (Online): 0493-2137
E-Publication: Online Open Access
Vol: 56 Issue: 06:2023
DOI 10.17605/OSF.IO/A8HW9

DIABETIC WOUND HEALING WITH ENHANCED ANTIMICROBIAL ACTIVITY AGAINST METHICILLIN-RESISTANT *STAPHYLOCOCCUS AUREUS* BY NATIVE *MENTHA PIPERITA* COPPER NANOPARTICLES

REEMA AFTAB, MS
Department of Biochemistry and Biotechnology, University of Gujrat, Hafiz Hayat Campus Gujrat, Punjab, Pakistan. Email: 16024379-003@uog.edu.pk

Dr. AMBER AFROZ, Ph.D.*
Assistant Professor, Department of Biochemistry and Biotechnology, University of Gujrat, Hafiz Hayat Gujrat, Punjab, Pakistan.
Corresponding Author Email: dramber.afroz@uog.edu.pk; ambernics01@gmail.com

NADIA ZEESHAN, Ph.D.
Department of Biochemistry and Biotechnology, University of Gujrat, Hafiz Hayat Campus Gujrat, Punjab, Pakistan. Email: nadia.zeeshan@uog.edu.pk

Abstract

Present research reports the enhanced diabetic wound healing potential of copper nanoparticles (CuNPs) synthesized from *Mentha piperita* obtained from high-altitude areas. Medioresinol was identified as a novel metabolite in *M. piperita* methanolic extract through Liquid chromatographic-tandem mass spectrometric analysis (LC-MS/MS). UV-vis and Fourier transform infrared spectroscopy confirm NPs with the presence of phenolic, amino, and ether groups. Spherical-shaped NPs with an average size of 100 nm were revealed by scanning electron microscopy. The bactericidal efficacy of CuNPs (2 mg/ml) against methicillin-resistant *Staphylococcus aureus* with an 18.3 mm inhibition zone was observed. CuNPs vividly possess antiglycation potential with 80% inhibition compared to *M. piperita* extract at 69%. Excision wounds were created on diabetic rats after receiving a single injection of alloxan monohydrate (150 mg/kg). One hour post diabetic induction, rats were treated with a topical formulation of CuNP-gel at 5-30mg/kg for 20 days and wound morphological parameters along with histopathological changes were evaluated. Conclusively, *M. piperita*-based CuNPs proved a critical role in wound epithelialization, proliferation, and differentiation with improved wound contraction in a dose-dependent manner, with 25 mg/kg as the best dose compared to positive and negative control groups. *M. piperita* metabolites enhanced the CuNP bactericidal and antidiabetic potential, along with wound healing activity *in-vivo* and *in-vitro*.

Keywords: Antibacterial, Diabetes, Medioresinol**,** *Mentha Piperita*, Nanoparticle, *Staphylococcus Aureus*, Wound Healing

List of Abbreviations: Copper nanoparticles (CuNPs); Bovine Serum Albumin (BSA), methicillin-resistant *Staphylococcus aureus* (MRSA), Liquid chromatographic-tandem mass spectrometric analysis (LC-MS/MS); Nanoparticles (NPs), advanced glycation end products (AGEs), Fourier transform infrared spectroscopy (FTIR), Haematoxylin and Eosin (H& E).

1. INTRODUCTION

Wound healing is a natural biological process that involves the restoration of damaged cells with the help of cytokines and growth factors [1]. The repair process consists of a series of molecular events aiming to establish functional integrity of damaged skin. Wound healing comprised of four progressive phases interacting in close vicinity [2]. During hemostasis, activated platelets coagulate the wound site by combining with fibrin protein to stop further bleeding [3]. Inflammatory mediators assist in engulfing debris and

Tianjin Daxue Xuebao (Ziran Kexue yu Gongcheng Jishu Ban)/
Journal of Tianjin University Science and Technology
ISSN (Online): 0493-2137
E-Publication: Online Open Access
Vol: 56 Issue: 06:2023
DOI 10.17605/OSF.IO/A8HW9

microbes from the wounded site and many growth factors release to recruit the migration of cellular components in the damaged area [4]. Proliferation is characterized by new blood vessel formation by vascularization of endothelial cells, granulated tissue formation, as well as the formation of fibronectin and fibroblast cross-linked with collagen with deposition of extracellular matrix. Epithelialization is marked by keratinocytes proliferation and fibroblast differentiation into myofibroblast to lessen the wound area [5]. Lastly, collagen matures and remodels to become tough skin. Wound restoration is a sophisticated process during which skin maintains itself after damage [2]. Numerous factors negatively impact the wound healing process. Diabetes is a complicated metabolic disorder, which distresses more than 340 million people globally, and results in diabetic wounds in approximately 20% of cases [6]. According to WHO: diabetes is said to be the 7^{th} leading cause of mortality by 2030. Diabetes-related fatalities account for more than 80% of all deaths worldwide and diabetic wounds account for 50 to 70% of limb amputations [7]. Diabetic patients have impaired glucose metabolism, which leads to hyperglycemia that worsens the healing process. The prevalence of poor restoration in diabetic patients is increasing worldwide because there aren't enough preventive and control measures. Delayed wound healing is the leading biomedical load on healthcare systems worldwide [8]. Diabetic leg and foot ulcers are two of the key issues associated with diabetic wounds. Diabetes impairs the healing process, which has a long-term negative effect on morbidity, mortality, and life quality. Diabetes affects each stage of wound healing. Diabetic wounds exhibit a prolonged inflammatory phase, reduced granulation tissue development, and decreased tensile strength at the injured site. This can be due to the vascular damage caused by ischemia [9]. Diabetes slows down the healing process which results in a non-healed, impaired wound along with numerous issues such as; psychiatric stress and depression, functional restrictions, trouble walking, cellulitis, abscess, osteomyelitis, gangrene, septicemia etc. The failure of wound healing in diabetes has been linked to altered cellular and metabolic components and activities [10]. The epigenetic code is altered by hyperglycemia and oxidative stress, which changes macrophage polarization and its regulation. Dysregulated polarizing macrophage contributes to the sluggish healing of wounds [11]. Numerous studies have demonstrated that diabetes is linked with sluggish wound healing, which is brought on by a challenging biochemical mechanism.

The evaluation of wound healing is a quite challenging process requiring continuous and systematic methods depending on the wound’s nature and severity. Despite years of research on wound healing, new medications still don't provide adequate results due to their high price, reduced efficacy, and side effects [12]. At present, impregnated wound dressings have been employed for wound treatment in animal and cell culture models [13-15]. Nanoparticles (NPs) such as silver, gold, iron, and zinc, etc. fascinate researchers worldwide and their excellent microbicidal potential owe to the fact that they can conveniently penetrate the cell membranes and cell walls of viruses and bacteria, thereby inhibiting protein synthesis, and destroy pathogen’s nucleic acids more efficiently compared to typical anti-fungal and anti-bacterial drugs [16]. Copper nanoparticles (CuNP) are amongst the most significant and widely utilized metal NPs, having a wide range of potential uses in nanotechnology. Cu is more affordable for a variety of

Tianjin Daxue Xuebao (Ziran Kexue yu Gongcheng Jishu Ban)/
Journal of Tianjin University Science and Technology
ISSN (Online): 0493-2137
E-Publication: Online Open Access
Vol: 56 Issue: 06:2023
DOI 10.17605/OSF.IO/A8HW9

applications compared to silver. Moreover, size, chemical stability, and conductivity make it stand out [17-19]. Cu is required in small quantities in many metabolic processes and depicts good antimicrobial and anti-inflammatory properties that make it a suitable candidate for immunity power, chronic healing, and skin remodeling therapies [20-22]. CuNP possesses enhanced catalytic activity and bioavailability as compared to native Cu. Metal NPs synthesized through chemical or physical means are not economical or safe for *in-vivo* application [13], thereby green medicine therapy can be utilized as a new strategy because it is cheap, reliable, effective, and safe to use. In the present research, we employed *M. piperita* leaves extract as a reducing and capping agent for CuNP synthesis. *M. piperita*; is a perennial herb from the Lamiaceae family, commonly known as peppermint with aromatic plants with simple, characteristic scented leaves that can be cultivated worldwide. It is a hybrid of spearmint (*M. spicata*) and water mint (*M. aquatica*), and possesses aromatic properties. Its leaves and essential oils are widely utilized in foods and as pharmaceutical products [23]. It provides relief to digestive disorders, gastritis, diarrhea, and skin disorders with itching, pain, and inflammation [24]. The pharmacological activities of its leaves are mainly accredited to polyphenols in them [25]. To the best of our knowledge, many studies report the green synthesis of gold and silver NPs for wound treatment. On the other hand, very few reports are available on plant-based CuNP for wound healing potential. In this study wound healing potential of *M. piperita*-based CuNPs is tested along with the exploration of novel phytoconstituents important in wound healing.

2. MATERIALS AND METHODS

2.1 Drugs and Chemicals

All the chemicals used were of analytic grade. Copper (II) sulfate pentahydrate ($CuSO_4 \cdot 5H_2O$; 99.5% purity), bovine serum albumin (BSA), methanol, glucose, ascorbic acid, potassium phosphate, trichloroacetic acid, Rutin, and alloxan monohydrate were from Sigma Aldrich, Polyfax was bought from GlaxoSmithKline, Pakistan.

2.2 Plant Collection

M. piperita from high altitude areas is collected, identified, and deposited in the National Herbarium of National Agricultural Research Centre (NARC), Islamabad under voucher # RAW100208. Afterward, it was cultivated in the botanical garden, and the Growth chamber of the Department of Biochemistry and Biotechnology, University of Gujrat, Gujrat Pakistan.

2.3 Extract Formation and Phytochemical Analysis

M. piperita leaves were plucked and washed thrice with autoclaved, distilled water and kept for shade drying for 15-20 days. Leaves were ground into a fine powder with a blade (food-grade stainless steel) grain miller 28,000/min and kept at 4°C. For extraction 50g leaves powder was immersed in 500 mL 80% (v/v) methanol and kept for gentle shaking at 37°C for 1D, followed by filtration using Whatman filter paper. Extracts were concentrated under reduced pressure at 40-50°C, in the rotary evaporator (Heidolph

Tianjin Daxue Xuebao (Ziran Kexue yu Gongcheng Jishu Ban)/
Journal of Tianjin University Science and Technology
ISSN (Online): 0493-2137
E-Publication: Online Open Access
Vol: 56 Issue: 06:2023
DOI 10.17605/OSF.IO/A8HW9

Rotary evaporator Laborata 4000 Sigma-Aldrich), and finally filtrates were placed at 4°C [26].

2.4 Mass Spectrometry

The phytochemical profiling of the *M. piperita* methanolic extract was performed by liquid chromatography-tandem mass spectrometry. Linear Ion Trap Mass spectrometer model; LTQ XL (ThermoElectron Scientific, USA) equipped with electrospray ionization (ESI) source and collision-induced dissociation (CID) (E range: 3-30) was used. Methanol was used as a solvent and the flow rate was adjusted to 10 µL/min. The ionization was with negative and positive scan modes with capillary voltage adjusted to 3.8 kV at 275ºC. The sheath and auxiliary gas flow rates were 20 and 5 units respectively. The mass range was (50-2000 *m/z*). Full-scan mass spectrum for the data at the *m/z* range was followed by an MS/MS experiment from the compounds of interest at 30% collision energy for 30 minutes. Calibration was performed by Xcalibur2.0.7. *M. piperita* leaves extract (20 mg) was solubilized in 5 mL of 10% methanol, loaded to the cartridge, and first eluted with the same solution. The 2nd and 3rd elution was with 5 mL of 50 and 90% methanol respectively. Fractions were dried under compressed air at 25ºC. The samples were dissolved in 100% methanol (Final Conc 10 ppm), and analyzed by mass spectrometry. All parameters were optimized to confirm greater ionization, and enhanced ion transfer, thereby achieving optimal signals of the precursor and fragment ions [27].

2.5 CuNPs Biogenic Synthesis

CuNPs were biologically synthesized using diluted extract (broth), where 30 mL leaf broth was mixed with 170 mL (1mM) $CuSO_4 \cdot 5H_2O$ solution to reduce copper ions. Mixtures were subjected to continuous shaking at 37ºC for 24h, and visually observed for the color change. Lastly, NPs were purified by repetitive centrifugation at 15000 rpm for 20 min followed by pellet dispersion in double distilled water and oven dried at 80ºC.

2.6 CuNPs Characterization

Apart from the color shift, CuNPs were further subjected to analytical techniques for the identification of their physical and morphological features. UV-spectrophotometer (UV-1800, Shimadzu UV Spectrophotometer) was employed for confirmation of the CuNP synthesis, which shows maximum absorption in the range of 500-550 nm. Fourier transform infrared spectroscopy (FTIR) analysis was carried out to identify possible functional groups (Thermo Fisher Scientific, NICOLET iS5, Japan). CuNPs' shape was analyzed by scanning electron microscope using (SEM) (FEI Nova Nano SEM 450).

2.7 Antibacterial assay

The bactericidal potential of CuNPs against methicillin-resistant *Staphylococcus aureus* (MRSA) was investigated by the disc diffusion method with some modifications [28]. Initially, the bacterial strain was grown in a sterile growth medium at 37°C with continuous shaking at 150 rpm for 12h, until the OD 600nm. Six different concentrations (0.5, 0.75, 1.0, 1.5, 2.0, and 2.5 mg/mL) of each sample were used. 10 µL sample was loaded on each disc and placed in LB plates. Ampicillin and DMSO were utilized as positive, and

Tianjin Daxue Xuebao (Ziran Kexue yu Gongcheng Jishu Ban)/
Journal of Tianjin University Science and Technology
ISSN (Online): 0493-2137
E-Publication: Online Open Access
Vol: 56 Issue: 06:2023
DOI 10.17605/OSF.IO/A8HW9

negative control respectively. Inhibitory zones around the discs were measured the next day.

2.8 Antiglycation activity

The antiglycation activity of *M. piperita* and its respective CuNPs was determined using a BSA assay with slight modifications [29]. Extract solutions were prepared in four concentrations (0.5, 0.75, 1.0, 1.5, 2, and 2.5 mg/mL). BSA (2 mg/mL) was incubated with 500 mM glucose solution at 37°C for 2 weeks, and fluorescent Advanced glycation end products (AGEs) were measured at 370nm following the emission at 440nm using a Nano Fluorometer. Lastly, 10 µL trichloroacetic acid (100% w/v) was added, followed by 10 min incubation at 37°C and centrifugation at 8,000× g for 3 min. The pallet thus obtained was dissolved in phosphate buffer saline. Rutin 2 mg/mL (20 mM) was used as a positive control. The percentage glycation inhibition for control, *M. piperita* extract, and CuNPs was calculated by the formula [29].

$$Inhibition\ (\%) = \frac{1 - Fluorescence\ of\ specimen}{Fluorescence\ of\ BSA/Glucose} \times 100$$

2.9 Animal Model

The present work was conducted after animal ethical approval from the University of Gujrat, Animal Ethics Committee (UOG/ORIC/2021/359). Healthy male albino rats around 200-250 g were used in the study. The animals were acclimatized at 22± 5°C with 12h cycles of light and dark; and given typical animal food to eat. Rats were subjected to starvation for 12h, followed by diabetic induction through a single intraperitoneal injection of alloxan monohydrate (150 mg/kg body weight) [30]. In order to reduce hypoglycemic shock, animals were provided with (5% w/v) glucose solution overnight. The body weight and fasting blood sugar level was checked on alternate days. Rats having a blood glucose level > 250 mg/dl were considered diabetic and employed for further experimentation [31].

2.10 CuNP-Carbopol gel formation

The CuNP-loaded gel was made using a carbopol polymer for topical application. The gel formulation was made with 10% Carbopol, 0.1 ml glycerine, triethanolamine, and CuNPs with continuous gentle stirring. Triethanolamine was added dropwise until pH 7 was achieved.

2.11 Wounds Induction and Treatment

After diabetic induction, rats were anesthetized with ketamine hydrochloride (30 mg/kg) prior to excision wound induction [32]. For excision wounds, the dorsal side of the rats was shaved, and an excision wound of 1×1 cm was created with a sharp surgical blade, and outlined.

2.12 Experimental Design

Rats were divided into eight groups; each containing 3 rats. *In-vivo* study design including animal grouping and treatment strategies are presented in (Tab. 1). All the formulations were topically applied daily until the scar fall off with complete healing. Wound

Tianjin Daxue Xuebao (Ziran Kexue yu Gongcheng Jishu Ban)/
Journal of Tianjin University Science and Technology
ISSN (Online): 0493-2137
E-Publication: Online Open Access
Vol: 56 Issue: 06:2023
DOI 10.17605/OSF.IO/A8HW9

contractions were measured on the 4, 8, 12, 16, and 20th day until complete healing. Percentage wound contraction [33] was calculated as follows:

$$Wound\ contraction\ (\%) = \frac{Initial\ wound\ size - specific\ day\ wound\ size}{Initial\ wound\ size} \times 100$$

Furthermore, epithelialization was monitored by assessing the days required for scar shedding without leaving an open wound area [34].

Table 1: *In- vivo* study design including animal grouping (Group I-VIII) and treatment strategies

Groups	Treatment strategies
I	Negative Control: diabetic untreated
II	Positive Control: administered topically with 30 mg/kg BWt of Polyfax ointment
III	Administered topically with 5 mg/kg BWt of CuNPs
IV	Administered topically with 10 mg/kg BWt of CuNPs
V	Administered topically with 15 mg/kg BWt of CuNPs
VI	Administered topically with 20 mg/kg BWt of CuNPs
VII	Administered topically with 25 mg/kg BWt of CuNPs
VIII	Administered topically with 30 mg/kg BWt of CuNPs

2.13 Histopathology

For histopathological studies, a portion of the healed skin from the wound center was excised on the 16th day and processed for microscopy. The animal tissues were fixed in neutral buffered formalin (10%) and transferred to (70%) ethanol [35-36]. Further, skin is processed, embedded in paraffin blocks, and 5 µm thick section was taken and stained by means of hematoxylin and eosin (H& E) for epithelialization and granulation, whereas Masson's Trichrome was done for collagen formation [37]. The stained samples were observed under the light microscope at 40x magnification.

2.14 Statistical analysis

Means of three replicates and standard deviation were calculated for all groups, and the data were subjected to one-way analysis of variance (ANOVA) and followed by Least Significant Difference (LSD) test for multiple comparisons using Graphpad Prism (9.3.0). Values of $p< 0.05$ indicated a statistical significance difference among the groups tested.

3. RESULTS

3.1 Phytochemical Profiling by LC-MS/MS

Chromatographic profiling is a convenient approach, as it provides preliminary information about the complexity and chemical composition of the peppermint extract. LC-MS/MS chromatographic profiles of the methanolic *M. piperita* extract are presented in (Fig. 1a-1e). Based on the MS database, 5 compounds from the *M. piperita* methanolic extract have been detected. ESI mass spectra in the negative mode were scrutinized for optimization and the data presenting main peaks with characteristic fragment ions, retention times, and calculated molecular masses are listed (Tab. 2).

Tianjin Daxue Xuebao (Ziran Kexue yu Gongcheng Jishu Ban)/
Journal of Tianjin University Science and Technology
ISSN (Online): 0493-2137
E-Publication: Online Open Access
Vol: 56 Issue: 06:2023
DOI 10.17605/OSF.IO/A8HW9

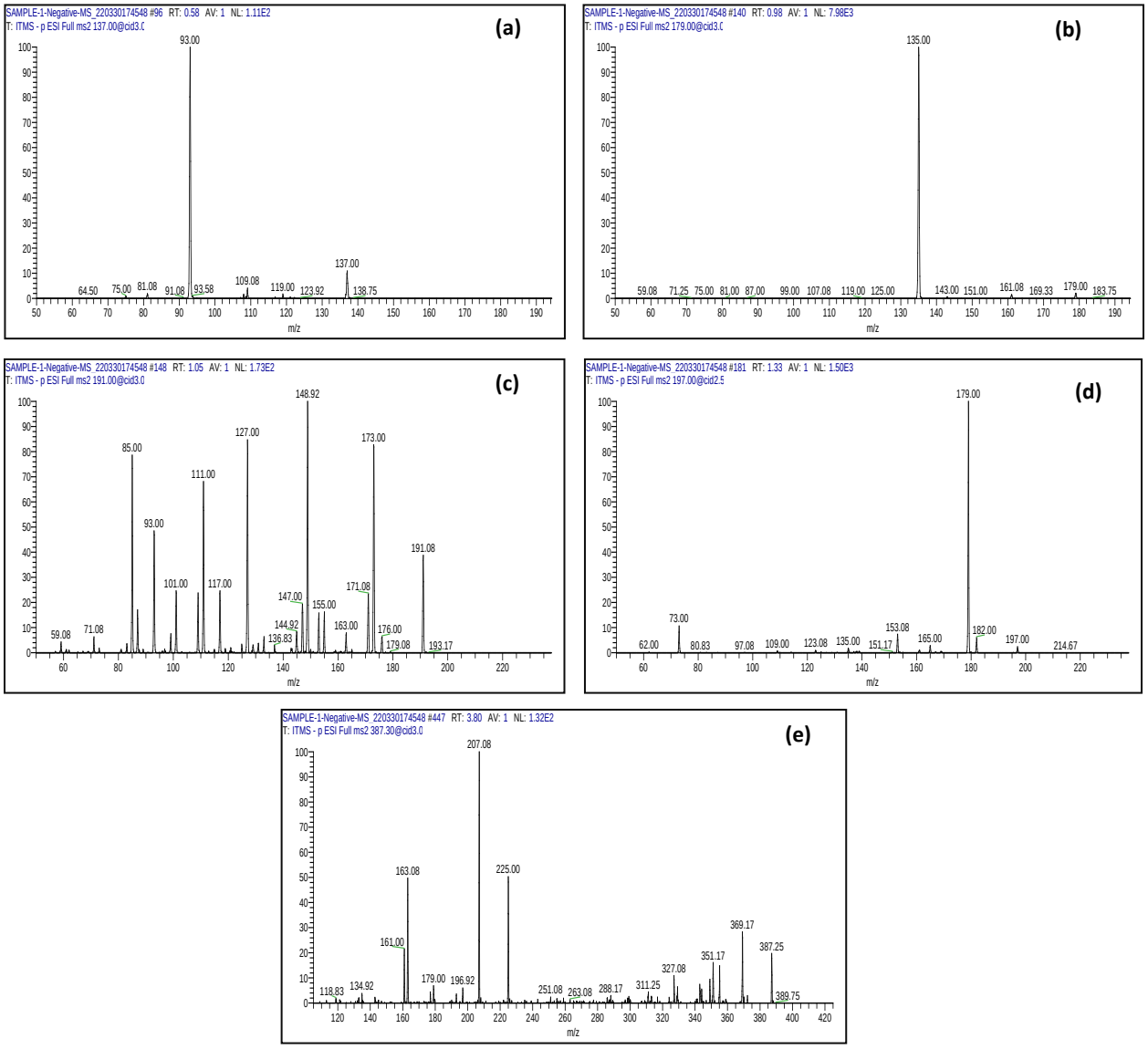

Figure 1: LC-MS/MS screening of peppermint methanolic extract: (a); p-Hydroxybenzoic acid, (b); Caffeic acid, (c); Citric acid, (d); Salvianic acid, and (e); Medioresinol

ESI-MS/MS data claimed Medioresinol was presumably identified at 387 m/z with fragmentation ions generated at m/z 387, 369, 351, 327, 225, 207, 163, 161, under negative ion mode. To the best of our knowledge, this metabolite is novel and has not been described before in this native *M. piperita* specie. Apart from the unique one, some other compounds have been identified as well. Further fragmentation ions at m/z 137, 179, 191, and 197, were presumably designated as p-hydroxybenzoic acid, Caffeic acid, citric acid, and Danshensu (Salvianic acid A) respectively.

Tianjin Daxue Xuebao (Ziran Kexue yu Gongcheng Jishu Ban)/
Journal of Tianjin University Science and Technology
ISSN (Online): 0493-2137
E-Publication: Online Open Access
Vol: 56 Issue: 06:2023
DOI 10.17605/OSF.IO/A8HW9

Table 2: Identified compounds in methanolic leaves extract of *M. piperita* by LC-MS/MS at negative ion mode

Peak	Retention Time (min)	$[M-H]^-$ m/z	Fragment Ions	Proposed Compounds
1	0.58	137	137, 93	p-Hydroxybenzoic acid
2	0.98	179	179, 135	Caffeic acid
3	1.05	191	191, 173, 171, 163, 155, 148, 147, 127, 117, 111, 101, 93, 85, 71	Citric acid
4	1.33	197	197, 182, 179, 153, 73	Salvianic acid A (danshensu)
5	3.80	387	387, 369, 351, 327, 225, 207, 163, 161	Medioresinol

3.2 CuNPs Characterization

Visual color shift served as the initial indicator of the synthesis. The addition of *M. piperita* extract to $CuSO_4 \cdot 5H_2O$ solution resulted in a color change from blue to greenish brown indicating the production of CuNPs (Fig. 2a). The CuNPs UV spectrum observed the broad band at ~550 nm, the surface Plasmon resonance (SPR) of CuNPs compared to crude *M. piperita* extract where no absorption band was observed owing to the lack of SPR (Fig. 2b). FTIR investigation evidences the different molecules present in *M. piperita* responsible for the CuNPs stabilization (Fig. 2c). Plant-based CuNPs exhibited the characteristic absorption bands at 3360 cm^{-1} confirming to the N-H stretching. A minor signal at 2108 cm^{-1} confirming to the C-N stretching. Intense band at 1635 cm^{-1} is credited to the carbonyl group responsible for NP synthesis. Another intense peak at 1347 cm^{-1} corresponding to the O-H bending and a small peak at 1015 cm^{-1} is recognized as C-O-C stretching vibration respectively. These results evidently confirmed the functional groups in plant extract; act as reducing, and capping agents for the CuNPs synthesis. The surface morphology of the CuNPs by SEM analysis at 500 nm magnification is shown in (Fig. 2d). SEM revealed spherical to irregular shaped nanomaterials with ~100 nm average size. The macromolecules encapsulating CuNPs' sustain the NPs agglomeration in layers, thereby tiny grains provide better opportunity to capture the size of the nanoparticle, thus agglomerating effect will be insignificant.

Tianjin Daxue Xuebao (Ziran Kexue yu Gongcheng Jishu Ban)/
Journal of Tianjin University Science and Technology
ISSN (Online): 0493-2137
E-Publication: Online Open Access
Vol: 56 Issue: 06:2023
DOI 10.17605/OSF.IO/A8HW9

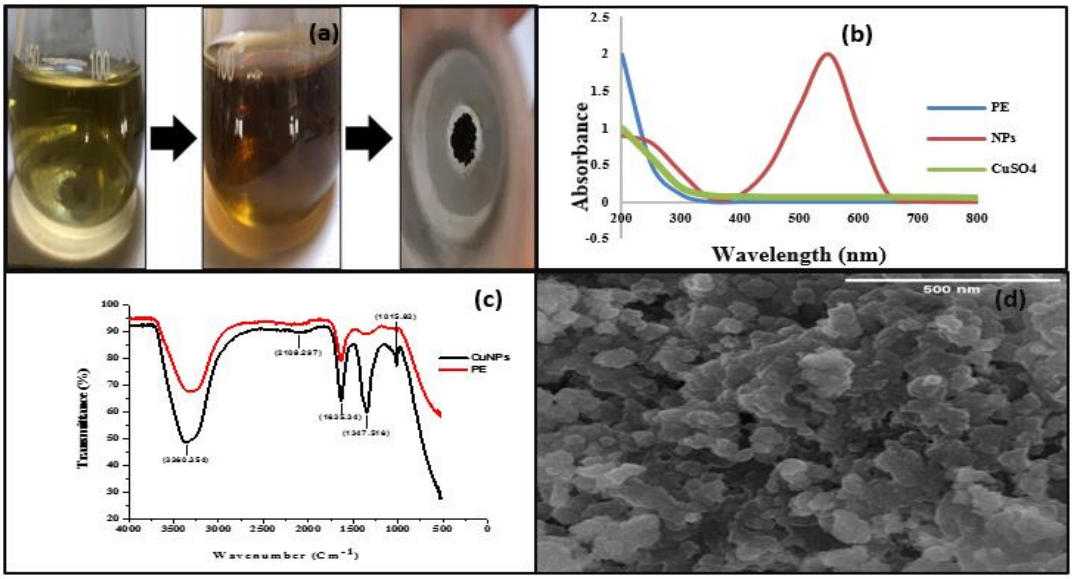

Figure 2: Characterization of CuNP synthesis: (a); Apparent color change in solution indicating CuNPs formation, (b); UV-Vis spectroscopic analysis of CuNP and *Mentha piperita* extract 24h-post-incubation, indicating synthesis of CuNP with the maximum absorption at 550 nm, (c); FTIR spectrum of CuNPs and peppermint extract showing probable functional groups, (d); SEM micrographs recorded for the CuNPs synthesized from peppermint extracts displaying nanostructures with spherical shape at 500 nm scale bar

3.3 *In-vitro* Antibacterial and Antiglycation Assays

CuNPs have shown significant antimicrobial activity against methicillin-resistant *Staphylococcus aureus* (MRSA). Zones of inhibition around each disc was measured subsequently (Fig. 3a). It has been observed that antibacterial potential increased with increasing concentrations with maximum inhibition were observed in case of highest concentration of 2 mg/mL and the least inhibition was observed with 0.5 mg/mL of each sample. The result of zone of growth inhibition by CuNPs was 18.3mm compared to the *M. piperita* extract i.e. 10.6 mm at 2 mg/mL against MRSA. Ampicillin (standard drug) possessed a maximum inhibitory zone, while DMSO (negative control) did not show any inhibition (Fig. 3b).

Tianjin Daxue Xuebao (Ziran Kexue yu Gongcheng Jishu Ban)/
Journal of Tianjin University Science and Technology
ISSN (Online): 0493-2137
E-Publication: Online Open Access
Vol: 56 Issue: 06:2023
DOI 10.17605/OSF.IO/A8HW9

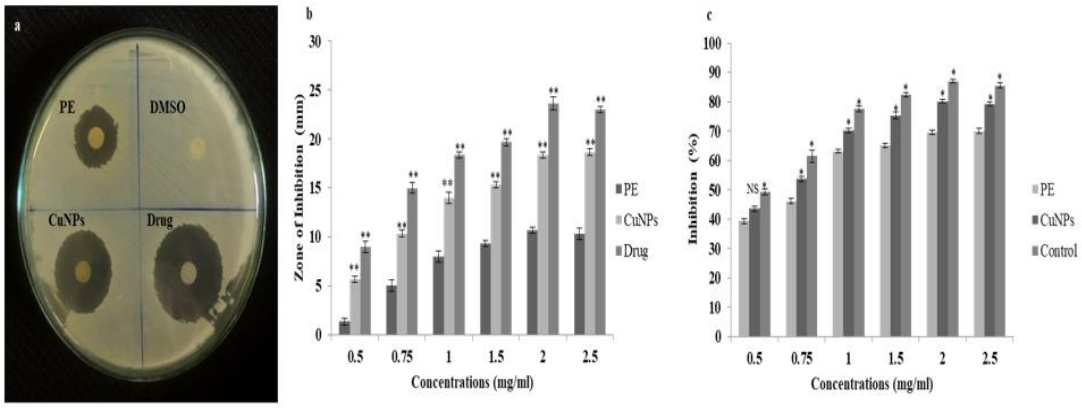

Figure 3: *In-vitro* biological activities: (a); Inhibitory zones against methicillin-resistant *Staphylococcus aureus* showing antibacterial activity, (b); Graphical representation of diameter of inhibitory zones (mm ±SD), (c); Graphical representation of percentage inhibition of glycation; (%±SD). P < 0.05 (*), P < 0.01 (**) when compared to control. PE=plant extract, CuNPs=copper nanoparticles

Herein inhibition of the formation of glycation reactions with *M. piperita* extract and CuNPs were explored to monitor the percentage inhibition of glycation between BSA, and glucose respectively The *in-vitro* antiglycation activity of *M. piperita* methanolic extracts and CuNPs was calculated at six different concentrations after 2 weeks of incubation (Fig. 3c). All the test samples depict inhibitory potential in a dose-dependent manner. It has been observed that reduced inhibition was shown by *M. piperita* extract (39%) and CuNPs (43%) at lowest concentration of 0.5 mg/mL. The strongest response was observed at the highest concentration (2 mg/mL) for *M. piperita* and resultant CuNPs. At 2 mg/mL *M. piperita* extract showed 69% inhibition, CuNPs displayed 80% inhibition, and maximum inhibition was shown by a standard drug (rutin) at 2 mg/mL. Over the course of 14 days, it was discovered that the fluorescence intensities of plant extracts and NPs were different at different doses. The extract and NPs with a concentration of 2 mg/mL were shown to form the least quantity of AGE compounds, hence exhibiting the highest inhibitory effect. The natural phenolic acid and flavonoid present in the *M. piperita* may attribute to such inhibitory effects.

3.4 *In-vivo* Wound Healing Activity

Wound contraction was observed macroscopically at different intervals (Fig. 4). CuNPs-gel-treated rats demonstrated significantly highest contraction in a dose-dependent manner (Fig. 4b) than all other groups. The least wound contraction was observed in the negative control (Fig. 4c), where pus formation with redness was observed. Wound closure was measured in terms of percentage contraction, maximum contraction in CuNPs-gel treated rats (97-98%) was observed at 25 & 30 mg/kg, compared to negative control with 69% contraction at 20D post-treatment, and took 29 days for complete healing (Tab. 3). Positive control showed 81% contraction which is slightly less than NPs treated animals 21D-post treatment was observed. Throughout the experiment, the control groups healing percentage was significantly lower than the experimental groups.

Tianjin Daxue Xuebao (Ziran Kexue yu Gongcheng Jishu Ban)/
Journal of Tianjin University Science and Technology
ISSN (Online): 0493-2137
E-Publication: Online Open Access
Vol: 56 Issue: 06:2023
DOI 10.17605/OSF.IO/A8HW9

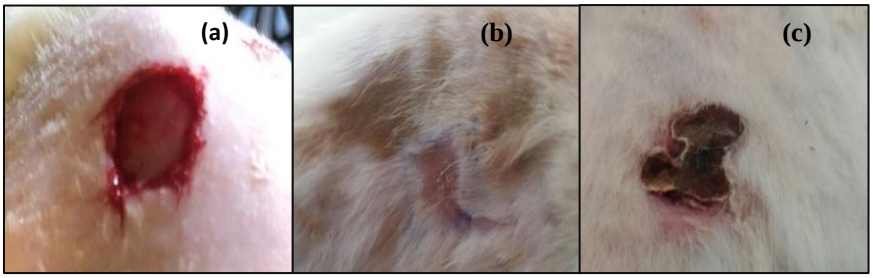

Figure 4: CuNPs accelerated wound healing in diabetic rats: (a; Rat on wound induction day, (b); healing of wound in CuNP-gel (25 mg/kg) treated rat at 16th day, (c); untreated rat

Rapid epithelization was observed in CuNPs treated animals at a dose of 25 & 30 mg/kg, which took 19D. Positive control took 24D for complete wound healing. While negative control healed slowly and took 29D to epithelize (Tab. 3).

Table 3: The post-wound contraction percentage and time of epithelization (days) after CuNPs-gel treatment at different doses (5mg/kg-30mg/kg) and compared with control groups

Groups	% Wound contraction after Days (Mean± SD with p < 0.05)					Epithelization time (Days)
	4	8	12	16	20	
I	5.16±1.04	10±0.70	22.3±2.51	38.33±1.52	69±4.00	29±1.00
II	9±1.00	17.83±1.60	32.86±3.0	53.2±2.83	81±1.00	24±1.00
III	7±1.00^{a}	17.6±1.52^{a}	31.6±1.52^{a}	46.3±1.52^{a}	71.3±1.52^{a}	27±1.00^{a}
IV	10.6±1.15^{a}	23.6±1.15^{b}	37±2.00^{a}	49±1.00^{a}	75.6±2.08^{a}	26±1.00^{a}
V	12±1.00^{b}	27±1.00^{b}	42.3±1.15^{b}	55.3±2.51^{b}	80±1.00^{b}	24±1.00^{b}
VI	14.33±0.57^{b}	31±1.00^{c}	49.3±1.52^{c}	60±2.00^{c}	86±1.00^{c}	22±0.00^{c}
VII	19±1.00^{c}	40±2.00^{d}	62.3±1.52^{d}	80±2.64^{d}	97±2.00^{d}	19±0.00^{d}
VIII	20.66±1.15^{c}	42.66±1.52^{d}	65.3±3.51^{d}	83.0±1.00^{d}	98±1.00^{d}	19±0.00^{d}

*Group I: **-ve** control (untreated+ undressed). Group II: **+ve** control: 30 mg/kg Polyfax ointment. Group III: CuNP-gel 5 mg/kg. Group IV: CuNP-gel 10 mg/kg. Group V: CuNP-gel 15 mg/kg. Group VI: CuNP-gel 20 mg/kg. Group VII: 25 mg/kg. Group VIII: CuNP-gel 30 mg/kg. Values with different superscripts in the same column differ significantly ($P < 0.05$).

3.5 Histopathological Study

Histopathological changes in experimental and control groups at the 16th-day post-wounding were observed after H & E and Masson's Trichome staining (Fig. 5). The most significant impact was seen with CuNP-Hydrogel, as it revealed a better histological image than Polyfax. Epithelization and tissue granulation was observed in all groups after H & E staining in 16th-day biopsies. Present work showed a better re-epithelization and moderate tissue granulation in rat tissues treated with CuNP (Fig. 5c1). CuNP treatment at a concentration of 25 mg/kg proved to be more effective in the regeneration of blood vessels together with fibroblast production. The positive control group also showed mild inflammatory infiltration, tissue granulation, and epithelization (Fig 5b1), while the negative control group showed incomplete healing with poor epithelization and tissue

Tianjin Daxue Xuebao (Ziran Kexue yu Gongcheng Jishu Ban)/
Journal of Tianjin University Science and Technology
ISSN (Online): 0493-2137
E-Publication: Online Open Access
Vol: 56 Issue: 06:2023
DOI 10.17605/OSF.IO/A8HW9

granulation (Fig. 5a1). In Masson's Trichome slides, CuNP treated group showed a presence of compact collagen fiber in numerous layers, and mild infiltration of polymorph leukocytes, along with thick epidermis, sebaceous glands, hair follicles, and little unhealed tissue (Fig. 5c2). Among control groups, positive control is characterized by less re-epithelization, and mild collagen fibers at the wound center (Fig 5b2), whereas in diabetic negative control incomplete healing with the absence of re-epithelization, and poor deposition of collagen fibers (Fig. 5a2).

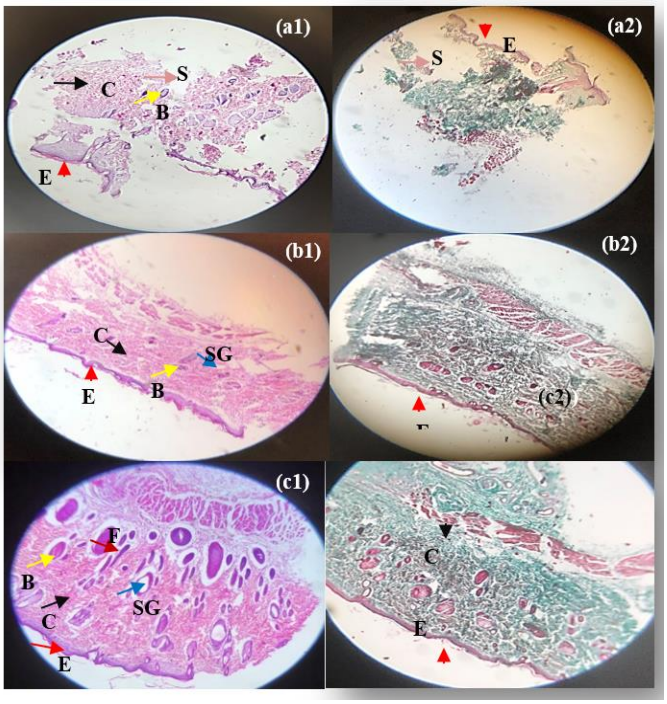

Figure 5: Histopathology of microscopic views of rat skin at 16th-day post wounding in different groups after (1) H& E and (2) Masson's Trichome staining at 400X. (a); Negative control, (b); Positive control, (c); CuNPs-gel (25 mg/kg) treated groups. SG: sebaceous glands, S: scab, C: collagen, F: Hair follicles, and E; Epidermal proliferation

4. DISCUSSION

Delayed wound healing is the leading biomedical load on healthcare systems worldwide [8]. Foot ulcers are the most prevalent wounds in people with diabetes. Diabetic patients have impaired glucose metabolism leads to hyperglycemia, which worsens the healing process. The prevalence of poor restoration in diabetic patients is increasing worldwide because there aren't enough preventive and control measures. To restore the skin's functional state and altered anatomical stability, wounds must be healed efficiently [38]. Faster contraction, enhanced epithelization, and a sufficient gain in tensile strength are important in rapid wound healing [39]. There are several natural phytochemicals being used as medicine today to treat post-diabetic problems with minimal side effects [40]. Patients with diabetes use herbal products almost everywhere without having information about their anti-inflammatory or anti-diabetic potential. The progressive effects of

Tianjin Daxue Xuebao (Ziran Kexue yu Gongcheng Jishu Ban)/
Journal of Tianjin University Science and Technology
ISSN (Online): 0493-2137
E-Publication: Online Open Access
Vol: 56 Issue: 06:2023
DOI 10.17605/OSF.IO/A8HW9

traditional treatments on diabetes and its related consequences, such as the development of diabetic foot ulcers and chronic wounds, had been documented in a variety of ethnobotanical literature. In the millennium's technological revolution, nanotechnology has become a major scientific field. In contrast to physical and chemical approaches, the scientific community had concentrated on the eco-friendly and highly effective green synthesis of metal NPs. Comparing medicinal plants to other living species, such as bacteria and fungi, it had been demonstrated that medicinal plants consist of numerous phytochemicals that can be employed for biogenic NPs production. Various metal NPs such as silver, gold, copper and zinc are excellent candidates for incorporation into wound dressings owing to their antibacterial capabilities and low toxic profiles [41]. In the current research, *M. piperita* methanolic leaves extracts are subjected to chromatographic profiling; as it is a useful approach that offers preliminary information about the complexity and chemical composition of the extract. LC-MS/MS analysis of *M. piperita* extract revealed major peaks associated with 5 bioactive compounds including, p-hydroxybenzoic acid, caffeic acid, citric acid, salvianolic acid, and medioresinol. Peaks data were in line with the literature [42-46]. Caffeic acid, rosmarinic acid, and medioresinol in rosemary had their role in obesity reduction and improved lipid profile [42]. Cherry stem containing caffeic acid, *p*-hydroxybenzoic acid, vanillin, *p*-coumaric acid, gallic acid, and ascorbic acid were detected by LC-MS/MS for their higher antioxidant and antimicrobial potential [43]. Phenols, flavonoids, gallocatechin, dimethyl ether, jaceidin, dihydro kaempferide, 12-hydroxy jasmonate sulfate, luteolin-*O*-rutinoside, and rosmarinic acid were major compounds in *Mentha*, and *Origanum majorana* extract [44-45]. *Salvia miltiorrhiza* root used in Chinese traditional medicine against heart, inflammatory diseases, and renal failure contains 58 compounds including hydrophilic phenolic, lipophilic diterpenoids, verbascose, salvianolic acid, caffeic acid, linoleic acid, linolenic acid, rosmarinic acid, and several organic acids by LC time of flight quadrupole MS [46]. To the best of our knowledge, Medioresinol is a novel compound present in this native *M. piperita* specie against diabetic wound healing. Each identified compound displayed a distinctive pattern of fragmentation, which result from the loss of hydroxyl, carboxylate, carbonyl, alkoxy, and a methyl group. During the ionization process, some substances are protonated and not fragmented completely. The protonated molecules tend to completely fragment as the collision energy rises. The applied collision energy was strongly correlated with the relative number of each fragment. Medioresinol belongs to the lignans, a class of phenolic compounds formed from two C6-C3 units or phenyl propanoids such as caffeic and ferulic acids. This compound appears to be found in the juice, seeds and wood of pomegranate, honey and other plants [47]. Many plants high in flavonoids have been used for thousands of years as food or herbal medicine since they serve a significant functional role in plant ecology and physiology [48]. The phenolic had been linked to a wide range of health advantages, including antibacterial, antioxidant, anti-diabetic, anti-inflammatory, anti-allergenic, anti-thrombotic, cardio-protective, and vasodilatory properties [49]. Numerous chemicals found in the *M. piperita* and identified in the present study had been reported to have antibacterial, antioxidant, anti-diabetic, and anti-inflammatory properties, indicating the possibility of using it for medical purposes. NPs synthesis by means of herbal extracts as bio-reductants and capping agents is advantageous over other synthesis approaches. CuNP synthesis was confirmed

Tianjin Daxue Xuebao (Ziran Kexue yu Gongcheng Jishu Ban)/
Journal of Tianjin University Science and Technology
ISSN (Online): 0493-2137
E-Publication: Online Open Access
Vol: 56 Issue: 06:2023
DOI 10.17605/OSF.IO/A8HW9

initially through color change and then through various analytical techniques. Our findings are consistent with other studies. The rapid changes in color owing to the surface Plasmon resonance (SPR) phenomenon [50]. The fabrication of CuNP from mint species was also reported; where the color of the copper sulfate aqueous solution, when mixed with extract solution begin to change from blue to pale light-brown [51]. The UV spectrum of CuNP observed the broad band at ~550 nm that is different from pure *M. piperita* extract where no absorption band was observed due to the lack of SPR. These findings are in the same line with the preceding studies [50, 52]. FTIR investigation evidences the different molecules found in plant extracts lead to the CuNPs stabilization. Based on FTIR analysis; functional groups' presence served as capping agents on NPs surfaces, preventing the agglomeration of metal NPs [53]. In the present study, spherical to irregularly shaped biogenic CuNPs were found by SEM. Our findings are in line with Iliger et al. [50], who reported cluster-shaped CuNPs with a size of more than 100 nm. In another study, spherical-shaped CuNPs with an average size of about 2.47 ± 1 μm were identified by Aderolu et al. [54]. The important marker in diabetic complications includes protein glycation and fructosamine formation called Amadori produces reactive methylglyoxal, deoxy glucose. Advanced glycation products formed includes further oxidation, dehydration; led to cellular dysfunction, memory loss, neuropathy, nephropathy, and retinopathy [55, 56]. Many ethnobotanical works have demonstrated the growing influence of the conventional treatments for diabetes. Although many important anti-glycation and anti-diabetic compounds had been isolated from several plants, there are still many practical plants currently used to treat post-diabetic complications not screened to identify bioactive compounds responsible for inhibitory activity [55]. CuNPs employed in this study have revealed the good percentage inhibition against the formation of fluorescent AGEs in a dose dependent manner. This trend is due to more consumption and doses that lead to increased oxidative stress and glycation rate that need to be further investigated. Plants and spices found in most homes may be able to stop the production of AGEs [56]. Present research implies that the combined interaction of phenolic compounds found in the extracts with nanomaterials could account for the antioxidant and antiglycation capabilities of domestic plants. Bactericidal potential of *M. piperita* extract, and CuNPs against Methicillin-resistant *Staphylococcus aureus* as investigated by disc diffusion assay. The antibacterial activity of NPs is best explained by their high surface area per volume and simple permeability [22]. The bactericidal properties of CuNPs are mainly attributed to copper cations released by CuNPs, attached to the bacterial cell wall with electrostatic attraction ultimately rupturing it, causing protein denaturation and dissipation of the proton motive force and cell lysis [57]. According to current studies, metallic CuNPs were more effective against several antibiotic-resistant bacterial strains, and more reactive than copper oxide NPs [54, 58]. The bactericidal capabilities of NPs suggest that they can be utilized as an effective alternative to antibiotics. The CuNPs therapeutic potential was tested for pronounced wound contraction and epithelialization. Biogenically synthesized CuNPs enhanced the wound healing more effectively than plant extract, and commercially available ointment. Morphological observation and histopathological examination of wound tissues further confirmed the superiority of the green synthesis approach. CuNPs intensified activity is endorsed to its strong antimicrobial potential that assists in the reduction of the microbial

Tianjin Daxue Xuebao (Ziran Kexue yu Gongcheng Jishu Ban)/
Journal of Tianjin University Science and Technology
ISSN (Online): 0493-2137
E-Publication: Online Open Access
Vol: 56 Issue: 06:2023
DOI 10.17605/OSF.IO/A8HW9

load at the wounded area and improves healing process [22, 59]. *M. piperita* based CuNP stimulate healing mechanism efficiently as it is rich in bioactive components such as essential oils, flavonoids, phenols that promote anti-inflammatory responses [24]. Phytochemicals may speed up the healing process by releasing oxygen anions and preventing peroxyl-free radicals [60]. Phytoconstituents in the *M. piperita* plays a part in the process of wound healing. The fibroblast linked to collagen deposition across healing wound area is indicator of recovery leading toward scar development. Fibroblasts are linked to the cytokines, interleukins secreted by macrophages involved in process of phagocytosis important in skin restoration. Less duration for tissue restoration by means of high collagen leading to scar formation are healing parameters [61-63]. The H&E staining show *M. piperita* based CuNP showed complete re-epithelialization 21D-post-wounding. MT staining also supports the observation of improved collagen deposition with granulation in CuNP-carbopol dressings made from *M. piperita*. The staining also shows thin dermis layer with rough epidermis in untreated diabetic model. The reason can be due to longer period of wound healing and closure might be attributed by longer duration of diabetic wound to achieve complete healing. The histological assay is in line with wound closure by *Moringa* leaf extract dressing [61]. Histopathology suggested carbopol dressings are capable to promote collagen deposition, with alignment to accelerate the wound contraction rate (Tab. 3; Fig. 5). Our work clearly disclosed novel compound; Medioresinol identified in *M. piperita* extract hold wound healing potential that could be an alternative source for wound healing therapies.

5. CONCLUSION

In this study, an ESI-MS/MS phytochemical fingerprint profiling of *M. piperita* methanolic extract revealed the detection of 5 compounds, among them Medioresinol is identified for the first time. Further we employed biomolecules mediated rapid, simple, and eco-friendly synthesis of CuNPs, as green synthesis approach has merits over other reported methods. Phenolic and flavonoids high content in the plant extract may be responsible for strong antimicrobial and antiglycation properties suggesting that the *M. piperita* together with CuNPs can be used as an effective wound-healing agent. A histological analysis of *M. piperita* based CuNPs-treated groups at the best dose of 25 mg/kg revealed better re-epithelialization, enhanced fibronectin content and fibroblast cells. It can be proposed that the further studies with purified constituents are needed to understand the complete mechanism of wound healing activity using plant extracts and CuNPs.

Acknowledgments

The authors would like to acknowledge Dr. Awais Asif; Nawaz Sharif Medical College, University of Gujrat, Hafiz Hayat Campus Gujrat, Punjab, Pakistan for antiglycation assays.

Declaration of Funding

This study is funded by National Research Program for Universities (NRPU 6506), Higher education Commission Islamabad, Pakistan at Department of Biochemistry and Biotechnology, University of Gujrat, Gujrat Pakistan.

Tianjin Daxue Xuebao (Ziran Kexue yu Gongcheng Jishu Ban)/
Journal of Tianjin University Science and Technology
ISSN (Online): 0493-2137
E-Publication: Online Open Access
Vol: 56 Issue: 06:2023
DOI 10.17605/OSF.IO/A8HW9

Data Availability Statement

All data generated or analyzed during this study are included in this published article [and its supplementary information files].

Conflict of interest statement

The authors declare no conflicts of interest.

Author Contributions

Experimental Design, Conceptualization, Funding source, Draft edition, Supervision [Amber Afroz]; Data creation, Investigation, Formal analysis [Reema Aftab]; Validation, Supervision, and Project administration [Nadia Zeeshan].

Ethical Statement

This study had been conducted with an animal ethical approval by the University of Gujrat Animal Ethics Committee, Office of research, innovation, and commercialization (ORIC) on ethical approval code UOG/ORIC/2021/359.

Consent for publication

Corresponding author had taken consent from all co-authors to submission and publication of their data in Tianjin Daxue Xuebao (Ziran Kexue yu Gongcheng Jishu Ban)/Journal of Tianjin University Science and Technology.

References

1. Borena B M, Martens A, Broeckx S Y, et al. Regenerative Skin wound healing in mammals: State-of-the-art on growth factor and stem cell based treatments [J]. Cell. Physiol. Biochem, 2015, 36: 1-23.
2. Wallace H A, Basehore B M, Zito P M. Wound healing phases. 2017.
3. Brown A. Phases of the wound healing process [J]. Nursing times, 2015, 111 (46): 12-13.
4. Komi D E A, Khomtchouk K, Santa Maria P L. A review of the contribution of mast cells in wound healing: involved molecular and cellular mechanisms [J]. Clinical reviews in allergy & immunology, 2020, 58: 298-312.
5. Raja K S, Garcia M S, Isseroff R R. Wound re-epithelialization: modulating keratinocyte migration in wound healing [J]. Frontiers in Bioscience-Landmark, 2007, 12 (8): 2849-2868.
6. Gregg E W, Sattar N, Ali M K. The changing face of diabetes complications [J]. The lancet Diabetes & endocrinology, 2016, 4 (6): 537-547.
7. Gupta A, Behl T, Sachdeva M. Key milestones in the diabetes research: A comprehensive update [J]. Obesity Medicine, 2020, 17: 100183.
8. Karimi K, Odhav A, Kollipara R, Fike J, Stanford C , Hall J C. A guide to early diagnosis and treatment [J]. Cutan. Med. Surg, 2017, 21: 425-437.
9. Catrina S B, Zheng X. Disturbed hypoxic responses as a pathogenic mechanism of diabetic foot ulcers [J]. Diabetes/Metabolism Research and Reviews, 2016, 32: 179-185.
10. Leung P. Diabetic foot ulcers—a comprehensive review [J]. The Surgeon, 2007, 5 (4): 219-231.
11. Mallik S B, Jayashree B, Shenoy R R. Epigenetic modulation of macrophage polarization-perspectives in diabetic wounds [J]. Journal of Diabetes and its Complications, 2018, 32 (5): 524-530.
12. Balekar N, Katkam N G, Nakpheng T, Jehtae K , Srichana T. Evaluation of the wound healing potential of Wedelia trilobata (L.) leaves [J]. Journal of Ethnopharmacology, 2012, 141 (3): 817-824.

Tianjin Daxue Xuebao (Ziran Kexue yu Gongcheng Jishu Ban)/
Journal of Tianjin University Science and Technology
ISSN (Online): 0493-2137
E-Publication: Online Open Access
Vol: 56 Issue: 06:2023
DOI 10.17605/OSF.IO/A8HW9

13. Borkow G, Gabbay J, Dardik R, et al. Molecular mechanisms of enhanced wound healing by copper oxide-impregnated dressings [J]. Wound Repair Regen, 2010, 18 (2): 266-275.

14. Abdollahi Z, Zare E N, Salimi F, Goudarzi I, Tay F R ,Makvandi P. Bioactive Carboxymethyl starch-based hydrogels decorated with CuO nanoparticles: antioxidant and antimicrobial properties and accelerated wound healing in vivo [J]. International Journal of Molecular Sciences, 2021, 22 (5).

15. Lemraski E G, Jahangirian H, Dashti M, et al. Antimicrobial double-layer wound dressing based on chitosan/polyvinyl alcohol/copper: in vitro and in vivo assessment [J]. International journal of nanomedicine, 2021, 16: 223-235.

16. Faúndez G, Troncoso M, Navarrete P , Figueroa G. Antimicrobial activity of copper surfaces against suspensions of Salmonella enterica and Campylobacter jejuni [J]. BMC microbiology, 2004, 4: 1-7.

17. Ghosh M K, Sahu S, Guptaa I, Ghorai T K. Green synthesis of copper nanoparticles from an extract of Jatropha curcas leaves: Characterization, optical properties, CT-DNA binding and photocatalytic activity [J]. RSC Advances, 2020, (37).

18. Lee H J, Song J Y, Kim B S. Biological synthesis of copper nanoparticles using Magnolia kobus leaf extract and their antibacterial activity [J]. Journal of Chemical Technology & Biotechnology, 2013, 88 (11): 1971-1977.

19. Yallappa S, Manjanna J, Sindhe M A, Satyanarayan N D, Pramod S N , Nagaraja K. Microwave assisted rapid synthesis and biological evaluation of stable copper nanoparticles using T. arjuna bark extract [J]. Spectrochim Acta A Mol Biomol Spectroscopy, 2013, 110: 108-115.

20. Tenaud I, Sainte-Marie I, Jumbou O, Litoux P, Dréno B. Invitro modulation of keratinocyte wound healing integrins by zinc, copper and manganese [J]. Brit J Dermatol, 1999, 140 (1): 26-34.

21. Sen C K, Khanna S, Venojarvi M, et al. Copper-induced vascular endothelial growth factor expression and wound healing [J]. American Journal of Physiology-Heart and Circulatory Physiology, 2002, 282 (5): H1821-H1827.

22. Borkow G, Gabbay J. Copper, An Ancient Remedy Returning to Fight Microbial, Fungal and Viral Infections [J]. Current Chemical Biology, 2003, 3: 272-278.

23. Sujana P, Sridhar T M, Josthna P, Naidu C V. Antibacterial Activity and Phytochemical Analysis of *Mentha piperita* L. (Peppermint)—An Important Multipurpose Medicinal Plant [J]. American Journal of Plant Sciences, 2013, 4 (1).

24. Giang J, Lan X, Crichton M, Marx W, Marshall S. Efficacy and safety of biophenol-rich nutraceuticals in adults with inflammatory gastrointestinal diseases or irritable bowel syndrome: a systematic literature review and meta-analysis [J]. Nutrition & Dietetics, 2022, 79 (1): 76-93.

25. Yahia I B H, Zaouali Y, Ciavatta M L, et al. Polyphenolic Profiling, Quantitative Assessment and Biological Activities of Tunisian Native *Mentha rotundifolia* (L.) Huds [J]. Molecules, 2019, 24: 2351.

26. Aftab R, Akbar F, Afroz A, Asif A, Khan RM, Rahman N, Zeeshan N. *Mentha piperita* silver nanoparticle loaded hydrocolloid film for wound restoration in diabetic rats and identification of bioactive compounds by ESI MS/MS analysis [J]. Journal of wound care, 2022, *Reference No.* Ref.: Ms. No. jowc.2022.0144R1.

27. Khan I, Rahman H, Abd El-Salam N M, et al. *Punica granatum* peel extracts: HPLC fractionation and LC MS analysis to quest compounds having activity against multidrug resistant bacteria [J]. *B*MC complementary and alternative medicine, 2017, 17: 1-6.

28. Thakur S, Tiwari K, Jadhav S. Antibacterial screening of root extract of Asparagus racemosus Willd [J]. Current Trends in Biotechnology and Pharmacy, 2015, 9 (2): 147-150.

29. Rasheed S, Sanchez S S, Yousuf S, Honore S M, Choudhary M I. Drug repurposing: In-vitro anti-glycation properties of 18 common drugs [J]. PloS one, 2018, 13 (1): 0190509.

Tianjin Daxue Xuebao (Ziran Kexue yu Gongcheng Jishu Ban)/
Journal of Tianjin University Science and Technology
ISSN (Online): 0493-2137
E-Publication: Online Open Access
Vol: 56 Issue: 06:2023
DOI 10.17605/OSF.IO/A8HW9

30. Kannur D M, Hukkeri V I, Akki K S. Antidiabetic activity of Caesalpinia bonducella seed extracts in rats. Fitoterapia, 2006, 77 (7-8): 546-549.

31. Idakwoji P A, Ekpo D E, Joshua P E, Njoku O U, Nwodo O F C. Ethanol extract of Tephrosia bracteolata leaves and its fractions ameliorates alloxan-induced diabetes and its associated complications in Wistar rat model [J]. International Journal of Diabetes in Developing Countries, 2021, 41: 456-468.

32. Massoud D, Fouda M M A, Sarhan M, Salama S G, Khalifa H S. Topical application of Aloe gel and/or olive oil combination promotes the wound healing properties of streptozotocin-induced diabetic rats [J]. Environmental Science and Pollution Research, 2022, 1-9.

33. Bardaa S, Makni K, Boudaouara O, et al. Development and evaluation of the wound healing effect of a novel topical cream formula based on Ginkgo biloba extract on wounds in diabetic rats [J]. BioMed Research International, 2021, 2021.

34. Kamath S, Rao S G, Murthy K D, Bairy K L, Bhat S. Enhanced wound contraction and epithelialization period in steroid treated rats: role of pyramid environment. 2006, 44: 902-904.

35. Elangbam C, Nyska A, Mahler B, Maronpot R. Heart trimming protocol of the laboratory rat [J]. Toxicologic Pathology, 2005, 33: 742.

36. Morawietz G, Ruehl-Fehlert C, Kittel B, et al. Revised guides for organ sampling and trimming in rats and mice--Part 3. A joint publication of the RITA and NACAD groups [J]. Exp. Toxicol. Pathol, 2004, 55: 433-449.

37. Chin C Y, Ng P Y, Ng S F. Moringa oleifera standardised aqueous leaf extract-loaded hydrocolloid film dressing: in vivo dermal safety and wound healing evaluation in STZ/HFD diabetic rat model [J]. Drug delivery and translational research, 2019, 9 (2): 453-468.

38. Frykberg R G, Banks J. Challenges in the Treatment of Chronic Wounds [J]. Adv. Wound Care, 2015, 4 (9): 560-582.

39. Ohno K, Kobayashi Y, Uesaka M, et al. A computational model of the epidermis with the deformable dermis and its application to skin diseases [J]. Scientific reports, 2021, 11 (1): 1-11.

40. Sen S, Chen S, Wu Y, Feng B, Lui E K ,Chakrabarti S. Preventive effects of North American ginseng (Panax quinquefolius) on diabetic retinopathy and cardiomyopathy [J]. Phytotherapy Research, 2013, 27 (2): 290-298.

41. Vijayakumar V, Samal S K, Mohanty S, Nayak S K. Recent advancements in biopolymer and metal nanoparticle-based materials in diabetic wound healing management [J]. International journal of biological macromolecules, 2019, 122: 137-148.

42. Vaquero M R, Yáñez-Gascón M J, Villalba R G, et al. Inhibition of gastric lipase as a mechanism for body weight and plasma lipids reduction in Zucker rats fed a rosemary extract rich in carnosic acid [J]. PloS one, 2012, 7 (6): 1-12.

43. Bursal E, Koksal E, Gulçin I , Bilsel G, Goren AC. Antioxidant activity and polyphenol content of cherry stem (*Cerasus avium* L.) determined by LC–MS/MS [J]. Food Res. Int, 2013, 51: 66-74.

44. Kapp K, Hakala E, Pussa T, Orav A. Commercial peppermint (*Mentha×piperita* L.) teas: Antichlamydial effect and polyphenolic composition [J]. Food Res, 2013, 53: 758–766.

45. Taamalli A, Arráez-Román D, Abaza L, et al. LC-MS-based metabolite profiling of methanolic extracts from the medicinal and aromatic species *Mentha pulegium* and *Origanum majorana* [J]. Phytochemical analysis, 2015, 26 (5): 320-330.

46. Yang ST, Wu X, Rui W, Guo J, Feng Y. UPLC/Q-TOF-MS Analysis for Identification of hydrophilic phenolics and lipophilic diterpenoids from Radix *Salviae Miltiorrhizae* [J]. Acta Chromatographica, 2015, 27: 711-728.

Tianjin Daxue Xuebao (Ziran Kexue yu Gongcheng Jishu Ban)/
Journal of Tianjin University Science and Technology
ISSN (Online): 0493-2137
E-Publication: Online Open Access
Vol: 56 Issue: 06:2023
DOI 10.17605/OSF.IO/A8HW9

47. Bonzanini F, Bruni R, Palla G, Serlataite N, Caligiani A. Identification and distribution of lignans in *Punica granatum* L. fruit endocarp, pulp, seeds, wood knots and commercial juices by GC–MS [J]. Food Chemistry, 2009, 117 (4): 745-749.

48. Singh, M A Shushni, A Belkheir. Antibacterial and antioxidant activities of *Mentha piperita* L [J]. Arabian Journal of Chemistry, 2015, 8 (3): 322-328.

49. Vichapong J, Sookserm M, Srijesdaruk V, Swatsitang P, Srijaranai S. High performance liquid chromatographic analysis of phenolic compounds and their antioxidant activities in rice varieties [J]. LWT - Food Science and Technology, 2010, 43 (9): 1325-1330.

50. Ramyadevi J, Jeyasubramanian K, Marikani A, et al. Copper nanoparticles synthesized by polyol process used to control hematophagous parasites [J]. Parasitol Res, 2011, 109 (5): 1403–1415.

51. Iliger K S, Sofi T A, Bhat N A, et al. Copper nanoparticles: Green synthesis and managing fruit rot disease of chilli caused by Colletotrichum capsici [J]. Saudi Journal of Biological Sciences, 2021, 28 (2): 1477-1486.

52. Sierra-Ávila R, Pérez-Alvarez M, Cadenas-Pliego G, et al. Synthesis of copper nanoparticles using mixture of allylamine and polyallylamine [J]. Journal of Nanomaterials, 2015, 2015.

53. Naghmouchi S, Al-Zaban M I, Al-Zaben M, Alharbi N, Bahatheq A. Generation and characterization of silver nanoparticles in *Mentha pulegium* extract and evaluation of biological activities of the prepared extract [J]. Journal of Nanomaterials, 2022, 2022.

54. Aderolu H A, Aboaba O O, Aderolu A Z, Abdulwahab K O, Suliman A A, Emmanuel U C. Biological synthesis of copper nanoparticles and its antimicrobial potential on selected bacteria food-borne pathogens [J]. Ife Journal of Science, 2021, 23 (1).

55. Asif A, Zeeshan N, Mehmood S. Antioxidant and antiglycation activities of traditional plants and identification of bioactive compounds from extracts of *Hordeum vulgare* by LC–MS and GC–MS [J]. Journal of Food Biochemistry, 2020, 44 (9): e13381.

56. Ceriello A, Giugliano D, Quatraro A, Donzella C, Dipalo G, Lefebvre PJ. Vitamin E Reduction of protein glycosylation in diabetes: New prospect for prevention of diabetic complications [J]. Diabetes Care, 2009, 14 (1): 68-72.

57. Raffi M, Mehrwan S, Bhatti T M, Akhter J I, Hameed A, Yawar W. Investigations into the antibacterial behavior of copper nanoparticles against *Escherichia coli* [J]. Annals of microbiology, 2010, 60 (1): 75-80.

58. Akhavan O, Ghaderi E. Cu and CuO nanoparticles immobilized by silica thin films as antibacterial materials and photocatalysts [J]. Surface and Coatings Technology, 2010, 205 (1): 219-223.

59. Salvo J, Sandoval C. Role of copper nanoparticles in wound healing for chronic wounds: literature review [J]. Burns & Trauma, 2022, 10.

60. Panda S K. Assay guided comparison for enzymatic and non-enzymatic antioxidant activities with special reference to medicinal plants [J]. Antioxidant enzyme, 2012, 14: 382-400.

61. Chin C Y, Ng P Y, Ng S F. *Moringa oleifera* standardised aqueous leaf extract-loaded hydrocolloid film dressing: *in vivo* dermal safety and wound healing evaluation in STZ/HFD diabetic rat model [J]. Drug Delivery and Translational Research, 2019, 9 (2): 453-468.

62. Pormohammad A, Monych N K, Ghosh S, Turner D L, Turner R J. Nanomaterials in wound healing and infection control [J]. Antibiotics, 2021, 10: 473.

63. Gunasekaran T, Nigusse T, Dhanaraju M D. Silver nanoparticles as real topical bullets for wound healing [J]. Journal of the American College of Clinical Wound, 2012, 3 (4): 82-96.